Compression-Induced Phase Transitions in Water-Soluble Polymer Brushes: The *n*-Cluster Model

E. M. Sevick

Research School of Chemistry, The Australian National University, Canberra ACT 0200, Australia

Received November 13, 1997; Revised Manuscript Received March 5, 1998

ABSTRACT: We describe the compression of a water-soluble polymer brush which undergoes compression-induced phase transitions. The solution behavior of the polymer comprising the brush is described using the de Gennes "*n*-cluster" model which predicts a region of coexistence between dense and dilute phases. We show that compression of the brush can induce the formation of a dense coexisting phase or the elimination of a dilute phase. These compression-induced transitions give rise to discontinuites in compression force profiles, which can be measured experimentally using the surface force apparatus or the atomic force microscope.

I. Introduction

Surfaces which are modified by the adsorption or attachment of a water-soluble polymer are important to many applications. These applications include stabilization of aqueous colloidal dispersions and imparting biocompatibility to in vivo objects such as implants and drug delivery systems. Water-soluble polymers have been known to exhibit unusual bulk solution behavior; however, it is only in recent years that solution models have been proposed specifically for these polymers.[1−4] One of the recent theories which we focus upon in this paper is the "*n*-cluster" solution model of de Gennes,[1] which was proposed for aqueous solutions of PEO or poly(ethylene oxide). In this paper, we study the compression of a layer of end-tethered polymers which are described by the *n*-cluster theory and show that compression can induce a phase transition within the brush. We predict, to within scaling constants, the force required to compress such a brush from its natural (free) height, $H_{\text{uncompressed}}$ to an arbitrary height, $H < H_{\text{uncompressed}}$. These force profiles predict signatures of compression-induced phase transitions within the brush. Such force profiles are measurable by surface force apparatus (SFA) or atomic force microscopy (AFM). The compressive forces predicted here are directly relevant to colloidal stabilization in aqueous solution.[5] While the *n*-cluster solution theory was originally motivated by PEO experiments, it may well extend to other hydrogen bonding polymers such as poly(*N*-isopropylacrylamide) in water[6] or polyacrylates in apolar solvents.[7] Other solution theories may also be used within the formalism of this paper. A comparison of the theoretical predictions and the experimental force profiles might also be used to discriminate among solution models.

The de Gennes *n*-cluster model[1] describes the solution thermodynamics of a polymer−solvent mixture where the pairwise interaction of monomers is repulsive (i.e., the solvent is a good solvent) but where interactions among a larger group or cluster of $n > 2$ monomers is attractive. These attractive *n*-cluster interactions may reflect the formation of helices among two more or strands or the microaggregates detected in light scattering experiments on an aqueous solution of dilute PEO.[8,9] The *n*-cluster theory consists of an interaction (mixing) free energy, F_{int}, in units of kT per unit volume, cast as

$$F_{\text{int}} = \rho(\phi - \phi^n) + (1 - \phi)\ln(1 - \phi) \qquad (1)$$

where the mixing entropy is taken for chains of infinite degree of polymerization. The attractive interactions contribute $-\rho$ ($\rho > 0$) enthalpy per *n*-cluster, or $-\rho\phi^n$ to the free energy, and the $\rho\phi$ term recovers zero mixing enthalpy when $\phi = 1$, as dictated by convention. For $\rho > \rho_c \equiv n^{-1}[(n - 1)/(n - 2)]^{n-2}$, F_{int} exhibits a concave, unstable region, and demixing results in two bulk phases, one concentrated at ϕ_+ and another dilute at ϕ_-. The values of ϕ_+ and ϕ_- at coexistence are determined by the equilibrium conditions:[10] (i) equality of chemical potentials, $\mu(\phi_+) = \mu(\phi_-)$ where $\mu = \mathrm{d}F_{\text{int}}/\mathrm{d}\phi$, and (ii) equality of osmotic pressures, $\pi(\phi_+) = \pi(\phi_-)$ where $\pi = \phi\mathrm{d}F_{\text{int}}/\mathrm{d}\phi - F_{\text{int}}$. These conditions prescribe constructions, either Maxwell's equal area construction on the $\mu-\phi$ surface or the common tangent construction on the $F_{\text{int}}-\phi$ surface, which can be used to determine ϕ_+ and ϕ_-.

The bulk demixing predicted for *n*-cluster chains in solution also occurs for chains which are end-tethered to a surface and gives rise to a discontinuity in the concentration profile of the brush. A theoretical description of uncompressed (or free) water-soluble brushes in the *n*-cluster model was explored by Wagner et al.[7] using the self-consistent field (SCF) approach.[11,12] Misra et al.[13] studied planar polyelectrolyte brushes in poor solvents and Birshtein et al.[14] studied brushes made of polymers with mesogenic units. Both theoretical studies showed phase separation within the body of the brush. In this paper we use the same rigorous method to construct concentration profiles for *n*-cluster brushes, and we extend the method to calculate the compression phase diagram and free energy and force-compression profiles.

The remainder of the paper is organized in the following manner. In the next section we review the theoretical methods which provide the monomer concentration profile of a brush comprised of a polymer whose solution behavior follows a prescribed model. Using the *n*-cluster model and SCF predictions of concentration profiles, we predict the regions of phase coexistence for brushes of arbitrary grafting density and compression. We also show that while the simple

S0024-9297(97)01679-3 CCC: $15.00
Published on Web 05/02/1998

Alexander−de Gennes step profile model is unable to predict force proiles, this simple model still captures the scaling behavior of critical compression at which phases appear and disappear. In the next section we construct free energy and force−compression profiles which signature the compression-induced phase changes. These force predictions should relate directly to experimental measurements obtained with the surface force apparatus or atomic force microscope using polymers whose solution behavior is described by the *n*-cluster model.

II. The Compression Phase Diagram of an *n*-Cluster Brush

The polymer brush is modeled as follows. Each chain has an equal degree of polymerization, N, and monomer size $a = 1$ and is tethered uniformly on an inert planar surface with density σ. All distances in our problem are scaled with N: $z = Z/(Na)$ where Z is the perpendicular distance measured from the grafting plane and the scaled brush height is $h = H/(Na)$ where H is the actual height of the brush. The distance between closest tether points is always taken to be less than the natural radius of a chain; consequently, we investigate brushes with grafting densities in the range $0 < \sigma < 1$ where $\sigma^{-1} < N$.

A rigorous scheme for determining the monomer concentration profile of any brush whose interaction energy is given by $F_{\text{int}} = f(\phi)$ is the self-consistent field approach,[11,12] which is described briefly in this paragraph. Consider a single chain in an existing brush whose trajectory, $z(n)$ for $n = 1, 2, ..., N$, is the scaled distance from the grafting plane to each of the indexed monomers. The free energy of that chain is the local energy integrated over the monomers of the chain:

$$F = \int_0^N \mathrm{d}n \left[\frac{1}{2}\left(\frac{\mathrm{d}z}{\mathrm{d}n}\right)^2 + \frac{\mathrm{d}F_{\text{int}}}{\mathrm{d}\phi}\right] \tag{2}$$

where the first term in the integrand is the local stretching energy and the second term is the interaction energy of the monomer with the local concentration, $\phi(z)$. The trajectory, $z(n)$, which minimizes the free energy of the chain is the solution to

$$\frac{\mathrm{d}^2 z}{\mathrm{d}n^2} = \frac{\mathrm{d}}{\mathrm{d}z}\left[\frac{\mathrm{d}F_{\text{int}}}{\mathrm{d}\phi}\right] \tag{3}$$

with the boundary conditions $z(n = 0) = 0$ and $\mathrm{d}z(N)/\mathrm{d}n = 0$, corresponding to the tethering of one end of the chain and the absence of stretch at the free end of the chain. These energies hold for any chain in the brush, and consequently, each chain in the brush must have a trajectory which satisfies eq 3 and its boundary conditions. Furthermore, irrespective of the position of the free end of the chain $0 < z(N) < h$, the tethered end must reside at the grafting surface. In this way, the trajectory of the chain is analogous to the trajectory of a particle moving in a harmonic potential of the form $V = \lambda - Bz^2$, given by

$$\frac{\mathrm{d}^2 z}{\mathrm{d}t^2} = \frac{\mathrm{d}}{\mathrm{d}z}(V) \tag{4}$$

where the polymerization index n is equivalent to the time of flight t, and the harmonic potential is identified with the local monomer chemical potential:

$$V = \lambda - Bz^2 = \frac{\mathrm{d}F_{\text{int}}}{\mathrm{d}\phi} = \mu(z) \tag{5}$$

The constant B is $\pi^2/8$ by the equal time constraint of trajectories. Implicit to this treatment is the absence of "dead zones", i.e., regions within the brush where free ends are prohibited. From this equation, we can see that λ is the monomer chemical potential at the root of the brush, $\lambda = \mu(0)$, and that the monomer chemical potential follows

$$\mu(z) - \mu(h) = B(h^2 - z^2) \tag{6}$$

Since the chemical potential is a function of the local concentration only, eq 6 provides the form of the concentration profile for a brush with specified h and concentration at the brush tip, $\phi_h = \phi(h)$. The normalized brush height, h, is determined by the conservation of monomers

$$N\sigma = \int_0^H \mathrm{d}z\, \phi(z) \tag{7}$$

for a specified grafting density. For uncompressed brushes, the monomer concentration at the tip of the brush is zero, $\phi_h = 0$, while for compressed brushes, the concentration at the tip is nonzero and grows with the degree of compression.

Equations 6 and 7 are sufficient for determination of the brush concentration profile, $\phi = \phi(z)$, for any ϕ-dependent bulk interaction energy, F_{int}. In the case of a pairwise excluded volume solution model, e.g., $F_{\text{int}} = \nu\phi^2/2$, an analytic solution of eqs 6 and 7 yields the free brush profile, e.g., $\phi(z) = B(h^2 - z^2)/\nu$. However, for arbitrary forms of $F_{\text{int}} = f(\phi)$, a simple analytic determination of $\phi(z)$ is not always possible and a numerical solution is required, as in the case of the *n*-cluster model. The numerical solution method follows that of Wagner et al.[7] and is simply an integration of tabulated values from the solution model, F_{int}, as shown in Figure 1. From F_{int}, we numerically tabulate (ϕ,μ) for given model parameters, replacing regions of unstable mixing with a phase boundary which straddles concentrations ϕ_+ and ϕ_- according to Maxwell's construction. Next, we translate the μ tabulation by a constant δ where $\delta > 0$ is identified with the chemical potential at the brush tip, μ_h. According to eq 6, the tabulation $(\phi, \mu - \mu_h)$ is also the tabulation $(\phi, B(h^2 - z^2))$, i.e., a form of the concentration profile which is valid for a brush with tip concentration ϕ_h and arbitrary height. The magnitude of the translation, $\delta = \mu_h$, can be related to the osmotic pressure or force exerted on the tip of the brush, $\phi_h\mu_h - F_{\text{int}}(\phi_h)$. The concentration profile is made specific by (a) specification of brush height, h, or by (b) specification of grafting density and determination of brush height according to the numerical integration of eq 7.

This construction demonstrates that when demixing occurs within the body of the brush (i.e., when $\rho > \rho_c$), the concentrations which straddle the demixing boundary are the same as those in the bulk, ϕ_+ and ϕ_-. The location of the demixing boundary is changed when the brush is compressed or the grafting density is increased, but the values of ϕ_+ and ϕ_- remain unchanged. For an uncompressed brush, Wagner et al.[7] found the minimal grafting density required for the brush to exhibit a demixing boundary: σ_c is that grafting density at which the root concentration exceeds ϕ_-. Uncompressed or

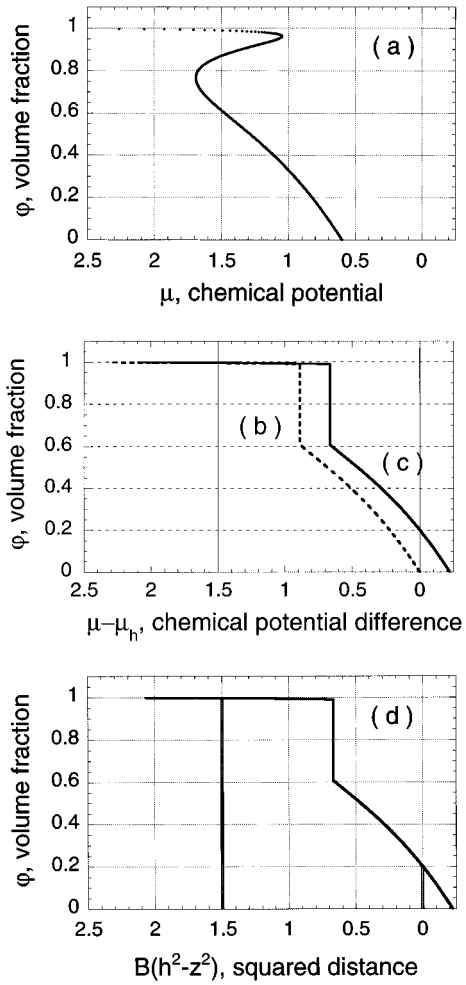

Figure 1. Numerical solution of monomer concentration profile for a brush comprised of polymer whose solution model is F_{int}. Shown is the method applied to the *n*-cluster model with $\rho = 0.4$ and $n = 10$. The chemical potential, $\mu = dF_{int}/d\phi$ is tabulated for monomer concentrations, ϕ (a). The unstable mixing region is eliminated and replaced with a demixing boundary straddling ϕ_+ and ϕ_- through Maxwell's construction. The resulting tabulation (b) is translated by an amount μ_h to obtain (c) which is identified with a monomer concentration profile (d) through eq 6. The tip of the brush ($z = h$) is found at $h^2 - z^2 = 0$ and the root of the brush ($z = h$) is determined from eq 7 and are specified by the broken lines on part d.

free brushes with grafting density below σ_c are comprised of a single phase with $\phi(z) < \phi_-$. For free brushes with grafting densities above σ_c, a demixing boundary separates a more dense phase near the root of the brush from a dilute phase on the tip side of the brush. As σ increases from σ_c, the location of the demixing boundary advances from the root of the brush, however the more dilute phase is always present at the tip for $\rho_c < \rho < 1$. As demonstrated by Wagner et al.,[7] at a sufficiently low temperature at which $\rho = 1$, the demixing concentration vanishes, $\phi_- = 0$. This corresponds to the disappearance of the dilute (good-solvent) phase such that the dense (poor-solvent) phase is in equilibrium with pure solvent at all grafting densities. Figure 2 shows the scaled brush height, $h = H/N$, as a function of the grafting density for characteristic model parameters which provide a wide window of phase coexistence, $\rho = 0.4$ and $n = 10$. Note that for grafting densities above σ_c, the brush height grows more slowly with grafting density as a growing fraction of monomers are incorporated into the growing dense phase.

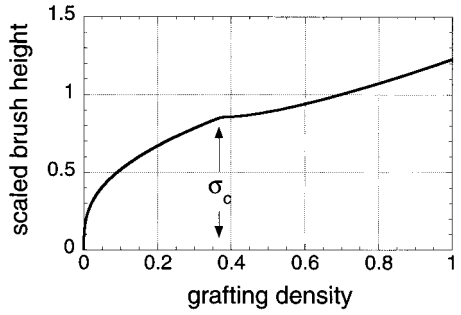

Figure 2. Scaled brush height, $h = H/N$, vs grafting density, σ, for an uncompressed (free) *n*-cluster brush with $\rho = 0.40$ and $n = 10$. $\sigma_c = 0.37$ is the smallest grafting density at which a coexisting dense (poor-solvent) phase is present. For grafting densities larger than σ_c, the brush height grows less strongly with grafting density. This is due to a growing fraction of monomers which are incorporated into the dense phase of the two-phase brush.

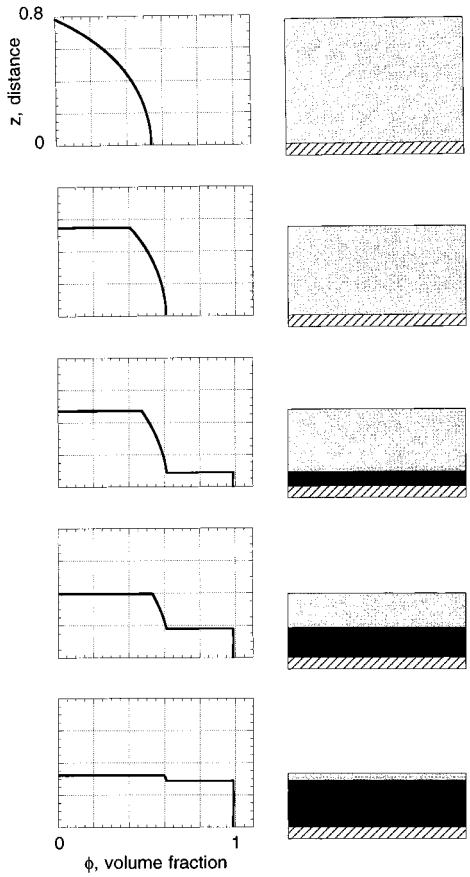

Figure 3. Monomer concentration profiles of an *n*-cluster brush which are compressed to 100 (free), 70, 60, and 40% of the free brush height. The profiles are provided as plots of the scaled distance from the grafting surface, $z = Z/N$, vs monomer volume fraction, ϕ, and were calculated using *n*-cluster parameters $\rho = 0.40$ and $n = 10$ with a grafting density of $\sigma = 0.30 < \sigma_c = 0.37$. Pictured opposite each profile is a schematic of the brush showing the proportion of dilute (light) and dense (dark) phases under compression.

Using the above numerical scheme, we can describe compression-induced demixing within brushes with grafting density below σ_c. A schematic of the brush compression is provided in Figure 3. The onset of the dense phase occurs with compression as compression increases the local concentration everywhere within the brush. When the concentration of the root of the brush exceeds $\phi(z = 0) > \phi_-$, then the dense phase results. With further compression, this collapsed phase grows

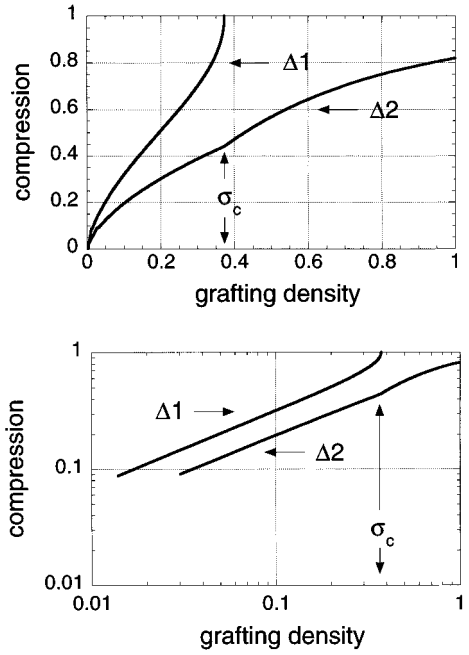

Figure 4. Locus of critical compressions for *n*-cluster brushes ($\rho = 0.40$, $n = 10$) with grafting densities between 0 and 1 plotted on linear (a) and log scales (b). The critical compression is the ratio $H/H_{\text{uncompressed}}$ associated with the onset of a coexisting, collapsed (poor-solvent) phase ($\Delta 1$) and the disappearance of the dilute (good-solvent) region leaving a single, dense (poor-solvent) brush, ($\Delta 2$).

in height, incorporating polymer monomers from the dilute phase. At strong compressions when $\phi_h = \phi_-$, all monomers have been incorporated into the collapsed root, and the brush is again in a single mixed phase, albeit a more dense, collapsed state. For brushes with grafting density above σ_c where phases coexist, compression causes the demixing boundary to advance toward the tip of the brush until the brush is wholly in the dense phase.

Figure 4 provides the loci of critical compressions which bound the phase coexistences at any grafting density ranging from $0 < \sigma < 1$. Compression is given as the ratio of heights in the compressed and free states, $0 < H/H_{\text{uncompressed}} < 1$ and the critical compressions, $\Delta 1$ and $\Delta 2$, correspond to compressions $H/H_{\text{uncompressed}}$ at which a coexisting phase appears and disappears, respectively. The compression profile of a brush of fixed grafting density corresponds to a vertical trace in Figure 4. For grafting densities $\sigma < \sigma_c$, compression transforms a brush (one phase) to a partially collapsed brush (two phase) and, with further compression, to a completely collapsed brush (one phase). For $\sigma > \sigma_c$, compression of the partially collapsed brush (two phase) reduces the number of monomers which are in the dilute phase until the volume of this phase disappears and the brush is completely collapsed (one phase). The character of the compressed phase diagram remains unchanged with different values of model parameters (ρ, n) as long as the interaction magnitude is larger than ρ_c and less than 1. With an increase in the interaction magnitude, ρ, the compression behavior occurs at lower grafting densities, as one would expect. Likewise, the attractive *n*-clustering leads to collapse regions at lower grafting densities for smaller values of n. Thus, weak attractive *n*-clustering, where n is large, provides a significant window of grafting densities and compression where phases coexist.

The compression phase diagram was constructed rigorously for the *n*-cluster solution model; however, we can understand the scaling behavior of the critical compressions $\Delta 1$ and $\Delta 2$ with grafting density using simple physical arguments based upon the Alexander−de Gennes model.[15] The Alexander−de Gennes model describes a simply solvated brush where the detailed concentration profile is replaced with a simple average monomer concentration. In simply solvated brushes, the SCF treatment reconstructs the same scaling laws as the simple Alexander−de Gennes picture. However, as pointed out by Wagner,[7] this simpler treatment is inappropriate for brushes in which there exists more than one solvation state or phase. In such brushes, the Alexander−de Gennes model predicts an unphysical discontinuity in pressure across the demixing boundary, and it is therefore necessary to use the full SCF treatment. However, the Alexander−de Gennes treatment should still be valid for *n*-cluster brushes under conditions where there is no internal demixing or under conditions of incipient demixing. Consequently, for uncompressed *n*-cluster brushes with grafting density below σ_c, where there exists only one phase, the height follows the well-known scaling form $H_{\text{uncompressed}} \approx \sigma^{1/3}N$. In the Alexander−de Gennes method, the critical compression, $\Delta 1$, would correspond to that compression at which the average concentration of the brush is increased to ϕ_-. Beyond this average concentration, a coexisting phase is created and the simpler scaling laws cannot be adopted. Since the brush volume per chain is $V = H/\sigma$ and the height is $H \approx V\sigma \approx N\sigma/\phi_-$, then the critical compression follows $\Delta 1 = H/H_{\text{uncompressed}} \approx \sigma^{2/3}/\phi_-$. Likewise, the critical compression, $\Delta 2$, corresponds to the maximum decompression at which the brush is not longer in the single, dense phase and the average concentration becomes less less than ϕ_+. This height is $H \approx V\sigma \approx N\sigma/\phi_+$ and the critical compression is $\Delta 2 = H/H_{\text{uncompressed}} \approx \sigma^{2/3}/\phi_+$. Both of these scaling forms are reproduced in the detailed SCF predictions at grafting densities lower than σ_c, Figure 4b. While the Alexander−de Gennes description, the simplest and least detailed model, captures the scaling of critical compressions with grafting density in single-phase brushes, it does not provide a physical description of compression within the coexistence region, and it cannot be used to predict force profiles. For these, SCF results are necessary.

III. The Free Energy and Force Profiles of Brush Compression

In this section we construct free energies and forces of an *n*-cluster brush over a continuous range of compression, $H/H_{\text{uncompressed}}$, following the SCF development put forth by Milner, Witten and Cates.[11] The free energy of a brush is the energy of chain addition, $\Delta F(\sigma)$, accumulated from zero grafting density to σ: $F = \int_0^\sigma d\sigma' \Delta F$. For a brush compressed to height h, the chains added at low grafting density will not "feel" the upper compression plane. Only when the grafting density reaches σ^*, the grafting density of a natural or uncompressed brush whose height is equivalent to the plate spacing, h, will the chains begin to feel compressed. Every chain added above σ^* is added under the constraint that the height is constant at the plate spacing and is less than the natural height of a free brush. Consequently, the tip concentration increases from $\phi_h = 0$ as the grafting density increases beyond σ^*. The free energy of the compressed brush is thus

$$F(\sigma,h) = \int_0^{\sigma^*} d\sigma' \, \Delta F + \int_{\sigma^*}^{\sigma} d\sigma' \, \Delta F \qquad (8)$$

The first term is the free energy of an uncompressed brush of height h; the second term is the accumulated energy of chain addition where tip concentration grows from 0 to ϕ_h. The free energy of addition of a tethered chain to an n-cluster brush is found from eq 2 and the harmonic potential equivalence, eq 6:

$$\Delta F = \int_0^N dn \left[\frac{1}{2}\left(\frac{dz}{dn}\right)^2 + \lambda - Bz^2\right] \qquad (9)$$

The chain trajectory, $z(n)$, which minimizes eq 9, satisfies the differential equation $d^2z/dn^2 - 2Bz = 0$ with the solution $z(n) = Q \sin(\pi n/(2N))$. Replacing this energy minimizing trajectory into eq 9 yields $\Delta F = \int_0^N dn \, \lambda = N\lambda = N\mu(0)$. Equation 8 reduces to

$$F(\sigma,h) = B \int_0^{\sigma^*} d\sigma' \, h^2 + \int_{\sigma^*}^{\sigma} d\sigma' \, \mu(z = 0) \qquad (10)$$

where it is understood that h in the first integrand is a function of σ' and that $\mu(0)$ in the second integrand is also a function of σ' and fixed height, h. Again, for simple F_{int} models, the right-hand side of eq 10 can be solved analytically; however the more general forms of $F_{int} = f(\phi)$ require numerical solution of the (ϕ, $\mu - \mu(h)$) or the (ϕ, $B(h^2 - z^2)$) tabulations of the previous section. The arguments of the first integrand on the right-hand side of eq 10 are found from a numerical integration of the tabulation which is translated by $\delta = \mu(\phi = 0)$, i.e., Figure 1b, using eq 7 to determine $h(\sigma')$ and σ'. The arguments of the second integrand are found from (ϕ, $\mu - \delta$) tabulations translated by successive increments $\delta > \mu(\phi = 0)$; each tabulation is numerically integrated according to eq 7 with fixed h to determine $\mu(0)$ and σ'. The numerical values of $F(\sigma,h)$ are sensitive to the level of discretization of the (ϕ, μ) tabulations as double integrations are required.

Figure 5 shows the free energy profile of an n-cluster brush under compression and at grafting density $\sigma < \sigma_c$ where the free brush is in the single, good-solvent phase. In this figure, the compression free energy of a simple pairwise excluded volume model, $F_{int} \approx f^2$, scaled to be equivalent to the n-cluster model under no compression, is included for comparison. With compression, the brush free energy always increases; however the n-cluster model exhibits discontinuities in slope, (dF/dH), which occur at the critical compressions which bound phase coexistence (Figure 4). Note that with initial compression, $1 < H/H_{uncompressed} < \Delta 1$, where the brush consists of a single good-solvent phase, the free energy increases in a manner similar to that for the simple, excluded-volume model. After the appearance of the dense, poor-solvent phase, the increase in free energy with compression is diminished; i.e., dF_{int}/dH is smaller, in comparison to that of the simple excluded-volume model. Indeed, Figure 5 shows that for compressions between $\Delta 1$ and $\Delta 2$, the free energy is almost linear with compression. More dense brushes, but with grafting densities still less than σ_c, also exhibit the diminished change in free energy with compression when the dense and dilute phases coexist. Noting that the dense phase is less compressible than the dilute, we may understand the compression free energy to be a result of the dilute, good-solvent phase alone: the dilute phase is continually being depleted of monomer as compression advances from $\Delta 1$ to $\Delta 2$, and consequently, compression of the remaining solvated monomers is energetically easier. When the dilute, good-solvent phase completely disappears at $\Delta 2$, further compression of the dense, poor-solvent phase requires significantly larger energy.

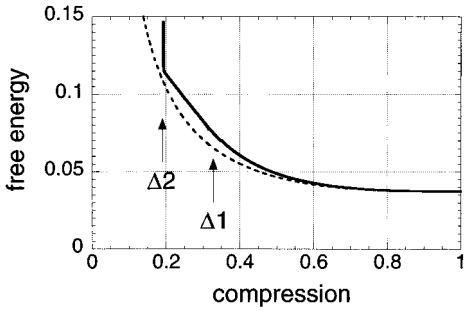

Figure 5. Free energy, F, vs compression, $H/H_{uncompressed}$ for an n-cluster brush ($\rho = 0.40$, $n = 10$) with grafting density, $\sigma = 0.1$ (full line) and for a simple pairwise excluded volume brush (dashed line). The n-cluster brush exhibits a nearly constant free energy slope for compressions between $\Delta 1$ and $\Delta 2$.

We have found the force vs compression curves that one could measure by compressing an n-cluster brush in the SFA or a specialized tip of an AFM. The compression force is equivalent to the osmotic pressure at the tip of the brush, which can be found from

$$f = -\phi_h (dF_{int}/d\phi)|_{\phi_h} + F_{int}|_{\phi_h} \qquad (11)$$

given the tip concentration, ϕ_h. Alternatively, the compression force can be determined as the derivative of the free energy with respect to brush height. However, one finds that the excessively fine discretization of the (ϕ, μ) tabulation which is required to eliminate numerical error in $dF/dH = f$ makes this latter method unattractive—except to provide a cross-check for calculation consistency. Figure 6 shows the force vs compression for n-cluster brushes of fixed grafting densities, both above and below σ_c. The critical compressions at which phases appear and disappear are marked on the force profiles and correspond to those on the compression phase diagram, Figure 4, at the appropriate grafting density. The discontinuities in the slope of Figure 5, discussed in the previous section, are more clearly visible in the force profile for $\sigma = 0.1$. Note that the brush becomes significantly more compliant (df/dH is smaller) when phases coexist and is incompressible for compression beyond $\Delta 2$ where the brush is comprised of a single, dense, poor-solvent phase. At a slightly larger grafting density, $\sigma = 0.3$, which is still less than σ_c, the force profile is similar except that the span of compressions over which phases coexist is greater and except that the brush is less compliant in this region but still more pliable than the single, good-solvent region, $1 < H/H_{uncompressed} < \Delta 1$. At $\sigma = 0.5$, i.e., where the grafting density is above σ_c, the dense and dilute phases coexist in the free brush. Compression depletes the dilute phase until $\Delta 2$, beyond which the brush becomes more incompressible. Note that the force required to compress and to deplete completely the dilute phase is independent of grafting density as one would expect from the invariant ϕ_+ and ϕ_-.

IV. Discussion

In this paper we have discussed the compression of brushes comprised of polymers which are water-soluble,

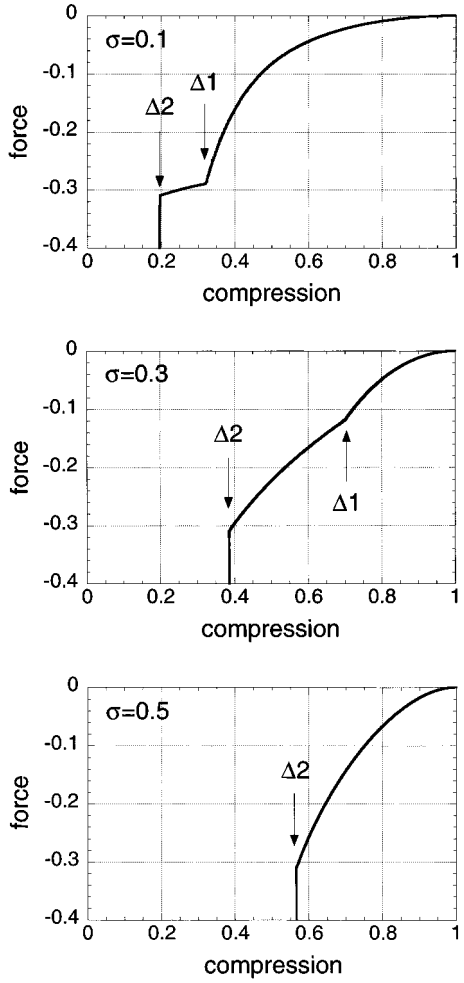

Figure 6. Compression profiles, force vs compression, for *n*-cluster brushes ($\rho = 0.40$, $n = 10$) with grafting densities (a) $\sigma = 0.1$, (b) $\sigma = 0.3$, and (c) $\sigma = 0.5 > \sigma_c$ which fingerprint the appearance/disappearance of coexisting phases.

using the de Gennes *n*-cluster model. We find that compression in brushes with grafting density smaller than σ_c can induce a coexisting dense phase at the root of the brush. With further compression, the phase boundary separating the phases advances from the root of the brush to the tip of the brush until the entire brush is comprised of the dense phase. The force required to compress the brush at grafting densities $\sigma < \sigma_c$ signals the appearance and disappearance of coexisting phases. At zero to small compressions, before the dense phase is induced, the force profile appears similar to that of a good solvent; i.e., the brush becomes less compliant with compression. However at the critical compression at which the coexisting dense phase appears, there is a discontinuity in the force profile and the brush becomes more compliant, particularly at smaller grafting densities. We understand this reduced growth in the force with compression as a result of the removal of monomers from the dilute phase to the coexisting dense phase which is less compressible. Indeed, when the second critical compression is attained, i.e., the compression at which all of the monomers reside in the dense phase, there is another discontinuity in the slope of the force. The force becomes very large with further compression, signifying the comparative incompressibility of the dense phase. For brushes of grafting density larger than σ_c, the free brush is comprised of coexisting phases and compression serves to eliminate the dilute phase at the tip of the brush. This compression behavior, shown in this paper for model parameters (ρ, n) = (0.4, 10) is characteristic of the *n*-cluster model for a range of parameters ($\rho > \rho_c$, n). For (ρ, n) = (0.4, 10), the coexisting phase at the brush root is very dense, i.e., ϕ_+ exceeds 0.90, giving rise to sharply incompressible regions in the force profiles. Other interaction parameters (ρ smaller and closer to ρ_c) yield smaller values of ϕ_+ and consequently the incompressibility of the brush for $H/H_{unocmpressed} < \Delta 2$ can be significantly reduced, but the discontinuities in the force profiles remain.

While the predictions of this paper focus upon the compression of one brush-lined plane with a bare, noninteracting plane, the results are also relevant to the compression between two brush-lined surfaces. The compression force profiles are relatively unchanged by the presence of the second brush whenever the brushes retain their dilute phases near the tip, i.e., whenever $H/H_{\text{uncompressed}} > \Delta 2$ (Figure 4), and whenever $\rho < 1$.[7] Under these conditions, the brushes are repulsive and oppose compression due to the lack of interpenetration of the solvated brush tip. However, whenever the dilute phase at the tip of the brush is absent, either through low temperature ($\rho > 1$) or large compression ($H/H_{\text{uncompressed}} < \Delta 2$), the brushes become less repulsive due to the attractive interactions of *n*-clusters that form between the two brushes. However, the binary interactions between brushes remain repulsive, and consequently, this effect may give rise only to a slight decrease in the repulsion between the brush-lined surfaces.

This paper focused upon polymers whose solution thermodynamics is modeled by de Gennes' *n*-cluster theory. However, the approach demonstrated here may be used in conjunction with other solution models, and comparison with experimental compression profiles from SFA or AFM may be used to discriminate among solution models. Indeed, the results of Misra et al.[13] and Birshtein[14] may also be viewed as tests for solution models of polyelectrolytes and mesogenic polymers, respectively. It is important to note, however, that SCF treatment used here implicitly assumes that there is no dead zone within the planar brush, either a free or compressed brush. It is unreasonable to rule out the possibility of dead zones, or regions of constant monomer composition, for general solution models. In addition, the SCF treatment also assumes lateral invariance; i.e., the monomer concentration varies only in the z -direction. However, evidence exists for lateral structure of tethered chains. For example, polymers weakly grafted and immersed in a poor solvent may form surface globules, referred to as "octopus" micelles.[16−18] Diblocks tethered over a range of grafting densities have been predicted to microphase separate to form surface micelles which might be used to laterally stripe or pattern a surface.[19,20] In cases where lateral microphase-separation or dead zones occur, the treatment used here is inappropriate and detailed SCF calculations[21] are required.

Acknowledgment. E.M.S. acknowledges the donors of the Petroleum Research Fund, administered by the American Chemical Society, for partial support of this research. The Research School of Chemistry is also acknowledged for award of a visitor's fellowship to Dr.

Avraham Halperin, who, during his short visit to ANU, inspired this work. He is also thanked for his discussions.

References and Notes

(1) de Gennes, P. G. *C. R. Acad. Sci. Paris II* **1991**, *313*, 1117.
(2) Bjorling, B.; Linse, P.; Karlstrom, G. *J. Phys. Chem.* **1990**, *94*, 471.
(3) Bekiranov, S.; Bruinsma, R.; Pincus, P. *Europhys. Lett.* **1993**, *24*, 183.
(4) Bekiranov, S.; Bruinsma, R.; Pincus, P. *Phys. Rev. E.* **1997**, *55*, 577.
(5) Napper, D. H. *Polymeric Stabilisation of Colloidal Dispersions*; Academic Press: London, 1983.
(6) Zhu, P. W.; Napper, D. H. *J. Colloid Interface Sci.* **1995**, *164*, 489. Zhu, P. W.; Napper, D. H. *Colloid Surf.* **1996**, *113*, 145.
(7) Wagner, M.; Brochard-Wyart, F.; Hervet, H.; de Gennes, P. G. *Colloid Polym. Sci.* **1993**, *271*, 621.
(8) Polik, W. P.; Burchard, W. *Macromolecules* **1983**, *16*, 978.
(9) Devanand, K.; Selser, J. C. *Nature* **1990**, *343*, 739. Boils, D.; Hair, M. L. *J. Colloid Interface Sci.* **1993**, *157*, 19.
(10) Landau, L. D.; Lifshitz, E. M. *Statistical Physics*; Pergamon Press: Oxford, England, 1980.
(11) Milner, S. T.; Witten, T. A.; Cates, M. E. *Europhys. Lett.* **1988**, *5*, 413; *Macromolecules* **1988**, *21*, 2610; *Macromolecules* **1989**, *22*, 853.
(12) Zhulina, E. B.; Borisov, O. V.; Pryanitsin, V. A. *Vysokomol. Soedin.* **1989**, *A31*, 185; *J. Colloid Interface Sci.* **1990**, *137*, 495.
(13) Misra, S.; Tirrell, M.; Mattice W. *Macromolecules* **1996**, *29*, 6056.
(14) Birshtein, T. M.; Amoskov, V. M.; Mercurieva A. A.; Pryamitsyn, V. A. *Macromol. Symp.* **1997**, *113*, 151.
(15) Alexander, S. J. *J. Phys. (Paris)* **1982**, *38*, 983; de Gennes P.-G. *J. Phys. (Paris)* **1976**, *37*, 1443.
(16) Williams, D. R. M. *J. Phys. Fr. II* **1993**, *3*, 1313.
(17) Zhulina, E. B.; Birshtein, T. M.; Pryamitsyn, V. A.; Klushin, L. I. *Macromolecules* **1995**, *28*, 8612.
(18) Stamoulis, A.; Pelletier E.; Koutsos, V.; Vandervegte, E.; Hadzioannu, G. *Langmuir* **1996**, *26*, 3221.
(19) Zhulina, E. B.; Singh, C.; Balazs A. C. *Macromolecules* **1996**, *29*, 6338; *Macromolecules* **1996**, *29*, 8254.
(20) Sevick, E. M.; Williams, D. R. M. *Colloids Surf. A* **1997**, *129*−*130*, 387.
(21) Scheutjens, J. M.; Fleer, G. J. *J. Phys. Chem.* **1979**, *83*, 1619.

MA9716793